Preclinical Evaluation of ^{99m}Tc-EC20 for Imaging Folate Receptor–Positive Tumors

Joseph A. Reddy, PhD; Le-Cun Xu, PhD; Nikki Parker, BS; Marilynn Vetzel, BS; and Christopher P. Leamon, PhD

Endocyte, Inc., West Lafayette, Indiana

Our group previously reported on the synthesis and characterization of a novel ^{99m}Tc-based folate-peptide chelator called EC20. This agent was found to bind folate receptor (FR)–positive cells and tissues with high affinity and was deemed useful for radiodiagnostic applications. In this study, we investigated the effect of D-amino acid substitution within EC20 on its tissue biodistribution. Expanded in vivo studies were also performed with unmodified ^{99m}Tc-EC20 to determine the effect of tumor FR expression, tumor size, tumor location, route of dose administration, and rodent diet on the agent's tissue biodistribution pattern. **Methods:** EC20 and EC53, the all-D-isomer of EC20, were synthesized and radiolabeled with ^{99m}Tc. The relative affinity of EC53 to the FR with respect to EC20 was then determined in cultured tumor cells. The ability of ^{99m}Tc-EC20 and ^{99m}Tc-EC53 to target tumors in vivo was examined using BALB/c mice with subcutaneously inoculated M109 or 4T1 cells, yielding 0.1- to 0.5-g tumors in 20 d. **Results:** The D-amino acid substitutions of EC20 were found to reduce the uptake of the agent into tumor and major organs. Subsequent studies using the original ^{99m}Tc-EC20 agent confirmed that its net tumor uptake was specific and proportional to FR expression levels in tumor cells as well as linear with respect to the overall tumor size. Further, ^{99m}Tc-EC20 uptake was found to be independent of both solid tumor location (intraperitoneal vs. subcutaneous) and the route of administration (intraperitoneal vs. intravenous). Interestingly, leucovorin supplementation of a commonly used folate-deficient laboratory chow had no effect on the agent's overall tissue biodistribution pattern. But, tumor-to-nontumor ratios could be increased up to 2.7-fold when 1 equivalent of free folic acid was coinjected with ^{99m}Tc-EC20. **Conclusion:** Taken together, these results confirm that ^{99m}Tc-EC20 has the potential to be a clinically useful noninvasive radiodiagnostic agent for detecting the locus of FR–positive cancers.

Key Words: folate receptor; tumor targeting; endocytosis; ^{99m}Tc; tumor imaging

J Nucl Med 2004; 45:857–866

In the past decade a remarkable growth occurred in the development of radiolabeled molecules for scintigraphic imaging of tumors (*1,2*). One approach has been through the use of tissue-specific ligands to direct a radiolabeled chelate more specifically to sites of pathology. The folate receptor (FR), which is overexpressed by many primary and metastatic cancers (*3–5*), is an example of one system that can be successfully exploited for drug delivery (*6–14*). After initial reports of successful targeting of FR–positive tumors with a ^{67}Ga-deferoxamine-folate conjugate (*15,16*), an improved folate-based radioligand labeled with ^{111}In was introduced (*17,18*). Thus, phase I/II clinical trials of ^{111}In-diethylenetriaminepentaacetic acid-folate (^{111}In-DTPA-folate) were conducted at several U.S. sites for the imaging of FR–positive ovarian cancers. Although encouraging tumor imaging and biodistribution data were obtained in humans, plans to commercialize ^{111}In-DTPA-folate were hampered by the high cost of ^{111}In and its suboptimal clinical applicability (i.e., long radiochemical half-life).

In contrast to ^{111}In-containing agents, ^{99m}Tc-based imaging agents are currently dominating the field of diagnostic nuclear medicine owing to their lower production costs and favorable nuclear characteristics (6-h half-life, 141-keV γ-rays) (*19*). The wide availability and cost effectiveness of ^{99m}Tc are also of major importance for routine clinical applications. Furthermore, it is now generally recognized that the rapid blood clearance and fast target localization properties of small molecule–based imaging agents are best used when short-lived radionuclides, such as ^{99m}Tc, are used (*19*). Thus, the impact of this clinical transition from ^{111}In to ^{99m}Tc prompted the creation of a variety of folate conjugate ^{99m}Tc-chelators, such as ^{99m}Tc-6-hydrazinonicotinamide (HYNIC) (*20*), ^{99m}Tc-ethylenedicysteine (*21*), and ^{99m}Tc-DTPA (*22*).

Our group previously reported on the development of an alternative peptide-based ^{99m}Tc-folate conjugate, referred to as ^{99m}Tc-EC20 (*23*). As a continuation of this work, we now report the results of more detailed preclinical performance evaluations. Thus, we investigated the effect of an all-D-amino acid substitution in the peptide fragment of EC20 on its in vivo distribution in a mouse model. The effect of tumor FR density and tumor size on ^{99m}Tc-EC20 tumor uptake was also explored. Further experiments were conducted to compare the biodistribution of intraperitoneal versus intravenous ^{99m}Tc-EC20 and on the accessible targeting of both subcutaneous and intraperitoneal FR–positive tumors. Finally, the ability to improve ^{99m}Tc-EC20's tumor-

Received Aug. 13, 2003; revision accepted Nov. 19, 2003.
For correspondence or reprints contact: Christopher P. Leamon, PhD, Endocyte, Inc., 1205 Kent Ave., West Lafayette, IN 47906.
E-mail: Leamon@endocyte.com

to-background contrast with coinjected versus preinjected folic acid was also investigated.

MATERIALS AND METHODS

General

N^{10}-Trifluoroacetylpteroic acid was purchased from Eprova AG. Peptide synthesis reagents were purchased from NovaBiochem and Bachem. ^{99m}Tc-Sodium pertechnetate was supplied by Syncor. Cellulose plates and diethylaminoethyl (DEAE) ion-exchange plates were purchased from J.T. Baker.

Synthesis, Purification, and Analytic Characterization of EC20 and EC53

EC20 is a folate-containing peptide consisting in sequence of pteroic acid (Pte), D-glutamic acid (D-Glu), β-L-diaminopropionic acid (βDpr), L-aspartic acid (L-Asp), and L-cysteine (L-Cys). EC20 was synthesized according to a previously described procedure (*23*). Briefly, using an acid-sensitive Wang resin loaded with fluorenylmethoxycarbonyl-trityl-L-cysteine (Fmoc-L-Cys(Trt)-OH), benzotriazole-1-yl-oxy-tris-pyrrolidino-phosphoniumhexafluorophosphate (PyBOP)-activated, protected amino acid monomers were sequentially applied. Fmoc protecting groups were removed after every coupling step under standard conditions (20% piperidine in dimethyl formamide). After the last assembly step, the peptide was cleaved from the polymeric support by treatment with 92.5% trifluoroacetic acid (TFA) containing 2.5% ethanedithiol, 2.5% triisopropylsilane, and 2.5% deionized water. This reaction also resulted in simultaneous removal of the *t*-butyl (*t*-Bu), *t*-butoxycarbonyl (*t*-Boc), and trityl protecting groups. Finally, the trifluoroacetyl moiety was removed in aqueous ammonium hydroxide to give EC20. EC53, the all-D-isomer of EC20, was similarly synthesized by replacing β-L-diaminopropionic acid (βDpr), L-Asp, and L-Cys with β-D-Dpr, D-Asp, and D-Cys, respectively. The crude EC20 and EC53 products were purified by high-performance liquid chromatography (HPLC) using an Xterra RP_{18} 30 × 300 mm 7-μm column (Waters) with a gradient mobile phase of 32 mmol/L hydrochloric acid and methanol. The structures of EC20 and EC53 were confirmed by ^{1}H nuclear magnetic resonance (NMR) spectroscopy. Chemical shifts and J values for EC20 (*23*) were similar to those of EC53. EC20 and EC53 were also analyzed by electrospray-mass spectrometry. Major positive ion peaks (m/z, relative intensity): 746.1 (M+H)+, 100; 747.1, 44; 556.8, 32; 570.8, 16.

Preparation of ^{99m}Tc-EC20/^{99m}Tc-EC53

EC20/EC53 kits are used for the preparation of radioactive drug substances. Each kit contains a sterile, nonpyrogenic lyophilized mixture of 0.1 mg of EC20 or EC53, 80 mg of sodium α-D-glucoheptonate, 80 mg of tin (II) chloride dihydrate, and sufficient sodium hydroxide or hydrochloric acid to adjust the pH to 6.8 ± 0.2 before lyophilization. Lyophilized powder is then sealed in a 5-mL vial under an argon atmosphere. Chelation of ^{99m}Tc to EC20 or EC53 is done by injecting 1 mL of ^{99m}Tc-labeled sodium pertechnetate (<1,800 MBq) into this vial and heating it for ~18 min in a boiling water bath. This solution can be stored at room temperature (15°C–25°C) protected from light, but it should be used within 6 h of preparation.

The radiochemical stability of the radioactive drug substances was determined by HPLC after storing at room temperature in a lead-shielded container for up to 24 h. Samples of ^{99m}Tc-EC20 and ^{99m}Tc-EC53 solutions were analyzed using an HPLC system consisting of a Waters 600E Multisolvent Delivery System and 490 ultraviolet (UV) detector, a Bioscan FC-3200 radiodetector, Laura 1.5 radiochromatogram software, and a Waters Nova-Pak C_{18} (3.9 × 150 mm) column. Injected samples were eluted with a linear gradient using an aqueous mobile phase containing 1%–50% solvent B (solvent A = 0.1% TFA in water; solvent B = acetonitrile) at a flow rate of 1 mL/min. The radiochemical purities of both ^{99m}Tc-EC20 and ^{99m}Tc-EC53 remained >90% for at least 24 h.

Determination of Radiochemical Purity of ^{99m}Tc-EC20/^{99m}Tc-EC53 by Thin-Layer Chromatography

The major radiochemical impurities in the preparation of ^{99m}Tc-EC20 and ^{99m}Tc-EC53 are (a) ^{99m}Tc-pertechnetate, (b) ^{99m}Tc-glucoheptonate (ligand exchange precursor), (c) nonspecific-binding ^{99m}Tc (^{99m}Tc bound at a site other than the expected Dap-Asp-Cys chelating moiety of the EC20 molecule), and (d) hydrolyzed ^{99m}Tc. Since ^{99m}Tc-EC20 was being tested for possible clinical use, a 3-thin-layer chromatography (TLC)–based method had been developed to determine the amounts of each impurity and to estimate the overall radiochemical purity.

In the first system a cellulose plate is developed with deionized water. Here, ^{99m}Tc-EC20/^{99m}Tc-EC53, ^{99m}Tc-glucoheptonate, nonspecific-binding ^{99m}Tc, and ^{99m}Tc- pertechnetate move to the solvent front (R_f = 1.0), while hydrolyzed ^{99m}Tc remains at the origin (R_f = 0.0). The cellulose plate is cut into 2 pieces at R_f = 0.3, and each piece is counted using a dose calibrator. The percentage of hydrolyzed ^{99m}Tc is calculated as follows: A = % hydrolyzed ^{99m}Tc = (kBq in bottom piece/kBq in both pieces) × 100.

In the second system, a cellulose plate is developed with acetone and 0.9% NaCl (7:3, v/v). ^{99m}Tc-Pertechnetate moves with R_f = 0.9, while ^{99m}Tc-EC20/^{99m}Tc-EC53, ^{99m}Tc-glucoheptonate, nonspecific-binding ^{99m}Tc, and hydrolyzed ^{99m}Tc remain at the origin (R_f = 0.0). The cellulose/acetone-saline plate is cut into 2 pieces at R_f = 0.6, and each piece is counted using a dose calibrator. The percentage of ^{99m}Tc-pertechnetate is calculated as follows: B = % ^{99m}Tc-pertechnetate = (kBq in top piece/kBq in both pieces) × 100.

Finally, in the third system, a DEAE ion-exchange plate is developed with 0.3 mol/L Na_2SO_4. ^{99m}Tc-Glucoheptonate moves to the solvent front (R_f = 1.0); nonspecifically bound ^{99m}Tc moves with R_f = 0.6; and ^{99m}Tc-EC20, hydrolyzed ^{99m}Tc, and ^{99m}Tc-pertechnetate remain near the origin (^{99m}Tc-EC20/^{99m}Tc-EC53, R_f = 0.1; hydrolyzed ^{99m}Tc, R_f = 0.0; ^{99m}Tc-pertechnetate, R_f = 0.3). The cellulose/Na_2SO_4 plate is cut into 2 pieces at R_f = 0.5, and each piece is counted using a dose calibrator. The percentage of ^{99m}Tc-glucoheptonate and nonspecific-binding ^{99m}Tc are calculated as follows: C = % (^{99m}Tc-glucoheptonate + nonspecific-binding ^{99m}Tc) = (kBq in top piece/kBq in both pieces) × 100. The overall radiochemical purity of ^{99m}Tc-EC20/^{99m}Tc-EC53 is then calculated as follows: Radiochemical purity = 100 – (A + B + C). The radiochemical purity of each ^{99m}Tc-labeled compound was determined by this 3-TLC–based method and, in all cases, was found to exceed 96% at the time of use.

Relative Affinity Assay

The relative affinity of EC53 was determined according to the method described by Westerhof et al. (*24*) with slight modification. Briefly, FR–positive KB cells were gently trypsinized in 0.25% trypsin in phosphate-buffered saline (PBS) at room temperature for 3 min and then diluted in folate-free RPMI medium (FFRPMI) containing 10% heat-inactivated fetal calf serum. After a 5-min 800*g* spin and one PBS wash, the final cell pellet was suspended

in FFRPMI 1640 (no serum). Cells were incubated for 15 min on ice with 100 nmol/L of ^{3}H-folic acid in the absence and presence of increasing concentrations of EC53. Samples were centrifuged at 10,000*g* for 5 min; cell pellets were suspended in buffer, transferred to individual vials containing 5 mL of scintillation cocktail, and then counted for radioactivity. Negative control tubes contained only the ^{3}H-folic acid in FFRPMI (no competitor). Positive control tubes contained a final concentration of 1 mmol/L folic acid, and counts per minute (cpm) measured in these samples (representing nonspecific binding of label) were subtracted from all samples. Notably, relative affinities were defined as the inverse molar ratio of compound required to displace 50% of ^{3}H-folic acid bound to the FR on KB cells, and the relative affinity of folic acid for the FR was set to 1.

Tissue Distribution Studies

Four- to 5-wk-old female mice (BALB/c strain) were purchased from Harlan Sprague–Dawley, Inc., and were maintained on a folate-free diet or leucovorin-supplemented folate-free diet for a total of 3 wk before the experiment. Syngeneic, FR–positive M109 tumor cells (1×10^6 cells per animal) or 4T1 tumor cells (2×10^5 cells per animal) were inoculated in the subcutis of the right axilla 3 wk before the experiment. Stock ^{99m}Tc-EC20 or ^{99m}Tc-EC53 solutions containing 100 μg of agent per milliliter were prepared on the day of use, and their radiochemical purities were >96%. All solutions were diluted with either saline alone or a saline solution containing 1 or 10 equivalents (eq.) of free folic acid such that the final radiopharmaceutical concentration was 10 μmol/mL.

Animals received an approximate 40 μmol/kg intravenous dose of test article in a 100-μL volume via a lateral tail vein during brief diethyl ether anesthesia. Alternatively, mice received intraperitoneal ^{99m}Tc-EC20 with a single bolus administration of test article in saline. Four hours after injection, animals were killed by CO_2 asphyxiation and dissected. Selected tissues were removed and weighed, and their radioactivity content was measured in an automatic γ-counter to determine ^{99m}Tc distribution. Uptake of the radiopharmaceutical in terms of the percentage injected dose of wet weight tissue (%ID/g) was calculated by reference to standards prepared from dilutions of the injected preparation.

FR Assay

A FR assay was performed according to Turk et al. (M.J. Turk, 2003), and all sample preparation procedures were performed at 4°C. Briefly, tissue samples were homogenized in homogenization buffer (10 mmol/L Tris, pH 8.0; 0.02 mg/mL each of leupeptin and aprotinin; 1 mL buffer per 50 mg of tissue). Membrane pellets were collected by centrifugation (40,000*g* for 60 min at 4°C) and resuspended in solubilization buffer (50 mmol/L Tris, pH 7.4; 150 mmol/L NaCl; 25 mmol/L *n*-octyl-β-D-glucopyranoside; 5 mmol/L ethylenediaminetetramethylene phosphonate; and 0.02% sodium azide). Insoluble material was removed by another centrifugation, and the total protein concentration of the supernatants was determined by the bicinchoninic acid protein assay method (Pierce Chemical Co.). Each sample was diluted to 0.25 mg/mL in solubilization buffer, and the solubilized FRs were concentrated by passing through Microcon-30 microconcentrators (30,000 molecular weight cutoff; Millipore Corp.). After a brief acid wash step to release endogenous folates, samples were neutralized and then allowed to bind ^{3}H-folic acid or ^{3}H-folic acid competing with 120 μmol/L unlabeled folic acid (25 mmol/L *n*-octyl-β-D-glucopyranoside; 350 mmol/L NaCl; 120 nmol/L ^{3}H-folic acid). The concentrators were washed 3 times with a detergent-based buffer (50 mmol/L *n*-octyl-β-D-glucopyranoside; 0.7 mol/L NaCl in PBS, pH 7.4). After the final wash, the retentates containing the solubilized FRs were recovered with PBS containing 4% Triton X-100. The samples were then counted in a liquid scintillation counter (Packard Bioscience Co.). Radioactivity values (cpm) were converted to picomoles of FR using the reagent's specific activity, and the final results were normalized with respect to the sample protein content.

RESULTS

Synthesis and Radiochemistry of EC20 and EC53, its All-D-Isomer

A peptide's biodistribution pattern can dramatically be affected by peptidase (serum, interstitial fluid, and tissue)-mediated degradation. One technique for achieving resistance to peptidases is through the use of D-amino acid residues within the peptide molecule. Therefore, to prevent the possible degradation of EC20 catalyzed by endogenous peptidases, its all-D-enantiomeric counterpart (EC53) was synthesized. Both EC20 and EC53 were built on solid supports applying Fmoc and Boc protection strategies. After the last assembly step, pteroyl-containing peptides were cleaved from the solid support and then deprotected by TFA treatment. The purities of EC20 and EC53 were >96% when tested by analytic HPLC (Fig. 1). The products were also characterized by NMR and electrospray-mass spectrometry, and the data were consistent with the expected structures of EC20/EC53, as illustrated in Figure 2.

Labeling of EC20 and EC53 with ^{99m}Tc was performed in alkaline aqueous medium using tin chloride. Incorporation of the radiotracer was practically quantitative within 20 min, and purities of >95% of ^{99m}Tc-EC20 or ^{99m}Tc-EC53 were commonly obtained. As shown in Figure 3, HPLC analysis of the ^{99m}Tc-EC20 and ^{99m}Tc-EC53 formulations showed 4 radiochemical components, designated as peaks A, B, C, and D. As described elsewhere (*23*), peak A was confirmed to be free ^{99m}Tc, which was typically present at <1% in both formulations. Peak B was assumed to be a ^{99m}Tc-EC20/^{99m}Tc-EC53 product chelated at a site other than the Dap-Asp-Cys position, and this specie represented <6% of the mixture in both products. In addition, peaks C and D (which accounted for the majority of the formulations) were confirmed to be diastereomers possessing either a syn- or anti-configuration about the technetium-oxygen bond in the Dap-Asp-Cys chelating ring (*23*). Furthermore, TLC analysis indicated that <2% of the radioactivity in the formulation was attributed to reduced, hydrolyzed technetium. As a consequence, no further purification was needed before use.

Binding Properties and Biodistribution of EC20 and EC53

Folate conjugates are typically analyzed using an in vitro relative affinity assay that measures a ligand's ability to directly compete with folic acid for binding to cell surface FRs. Thus, ^{3}H-folic acid is used as the radioligand, whereas unlabeled folic acid serves as the reference compound. We have previously reported that EC20 has a relative affinity

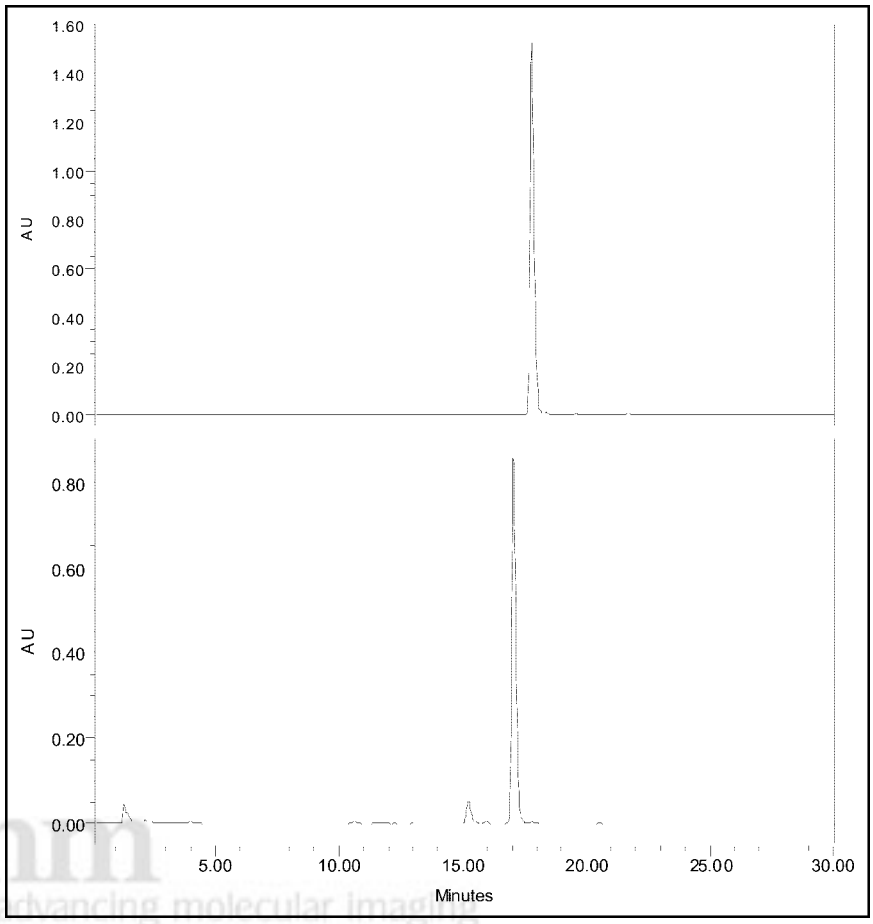

FIGURE 1. HPLC profiles of EC20 (Top) and EC53 (Bottom). Samples of EC20 or EC53 were analyzed on a Waters Nova-Pak C_{18} (3.9 × 150 mm) column using a 30-min linear gradient from 10% to 50% solvent B (solvent A = 0.1% TFA in water; solvent B = methanol) at a flow rate of 1 mL/min. AU = absorbance units.

value of 0.92 (*23*). As shown in Figure 4, EC20's all-D-isomeric counterpart, EC53, was determined to have a relative affinity value of 0.23. Although EC53's net affinity for the FR is lower compared with that of EC20, this new agent is still considered to be a moderately high-binding ligand.

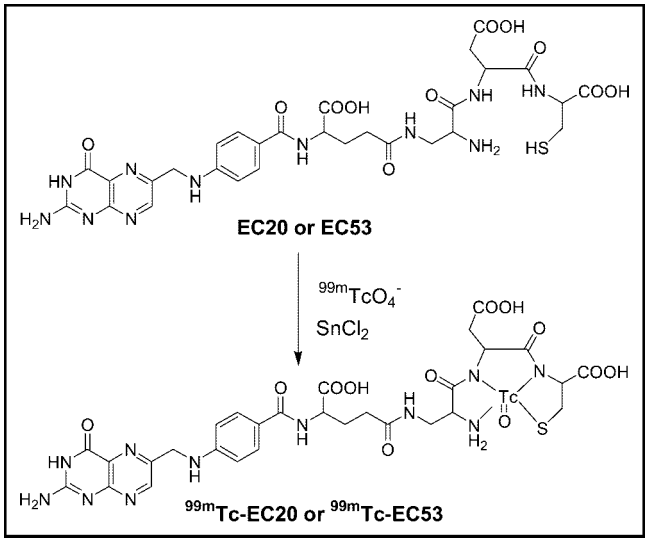

FIGURE 2. Formation of ^{99m}Tc-EC20 and ^{99m}Tc-EC53.

D-Amino acid replacement can possibly change the in vivo stability of the peptide portion because the cellular absorption, hepatic and renal clearance, and binding of protease to peptide may be affected by the interactions between peptide and various serum components. Hence, biodistributions of ^{99m}Tc-EC20 and ^{99m}Tc-EC53 were compared in BALB/c mice bearing subcutaneous FR–positive M109 tumors. Animals were dosed intravenously with the test articles, and selected organs were collected and counted for radioactivity 4 h later. Uptake was expressed as %ID/g tissue, and tumor-to-nontumor (T/NT) ratios were also calculated to assess the selective targeting of the agents.

As shown in Table 1, the highest tissue uptake with both agents was measured in the FR–positive tissues—namely, the tumors and kidneys. Relative to EC20, the D-amino acid substitutions in EC53 reduced its uptake in the kidneys and tumor by approximately 33%. T/NT organ ratios were also reduced with ^{99m}Tc-EC53 in all cases except the muscle, heart, and lung. Tissue counting data from animals given either agent showed <5 %ID/g of gastrointestinal tract tissue, suggesting that the primary route of radioactivity elimination from the body in each case was urinary. Since EC53 did not promote increased tumor uptake or enhanced T/NT ratios in most organs relative to EC20, it was concluded that endogenous proteolytic activity on EC20 was

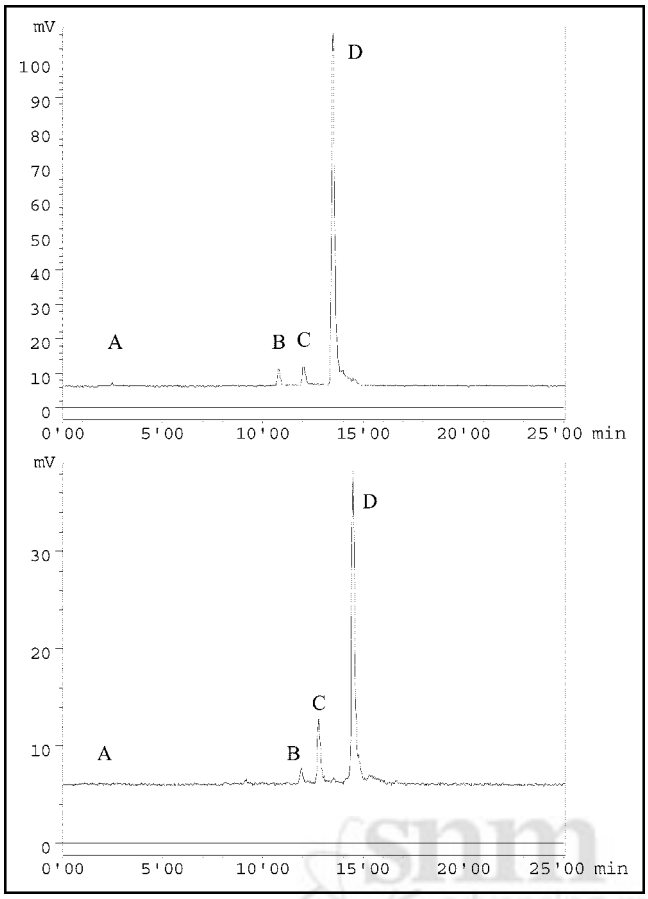

FIGURE 3. HPLC profiles of ^{99m}Tc-EC20 (Top) and ^{99m}Tc-EC53 (Bottom). Samples of ^{99m}Tc-EC20 or ^{99m}Tc-EC53 were eluted on a Waters Nova-Pak C_{18} (3.9 × 150 mm) column using a 30-min linear gradient from 1% to 50% solvent B (solvent A = 0.1% TFA in water; solvent B = acetonitrile) at a flow rate of 1 mL/min.

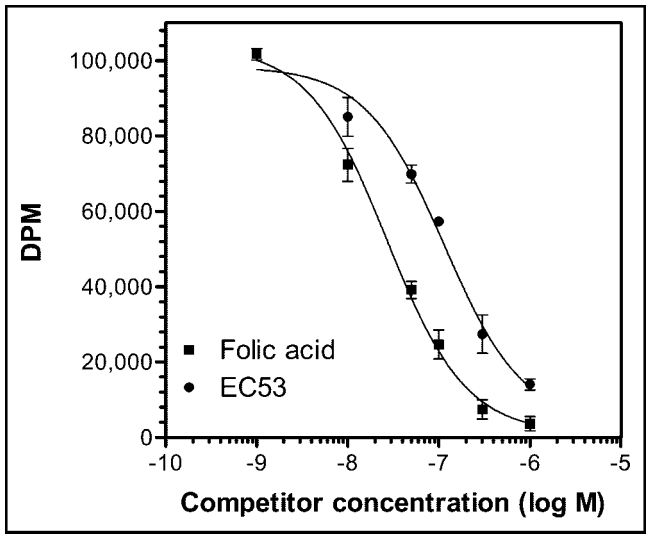

FIGURE 4. Competitive blocking of ^{3}H-folic acid binding to KB cells with EC53. KB cells were incubated for 15 min on ice with 100 nmol/L ^{3}H-folic acid in the presence and absence of increasing EC53 concentrations. Error bars represent 1 SD (n = 3).

probably insignificant. The fact that EC53 accumulated in kidney and tumor to a lesser degree than EC20 may have been due to EC53's slightly reduced affinity for the FR (Fig. 4). Thus, all remaining experiments were performed using the EC20 reagent.

Effect of FR Expression Level on ^{99m}Tc-EC20 Uptake by FR–Expressing Tumors

The mouse cell lines 4T1 and M109 reproducibly form tumors in BALB/c mice, and they express varying amounts of FR (1.6 and 95.5 pmol FR/mg membrane protein, respectively; Table 2). A third cell line was also generated by continuous culturing of 4T1 cells in growth medium containing very low levels (10 pmol/L) of folic acid. As expected, the growth of 4T1 cells in 10 pmol/L folic acid resulted in upregulated FR expression from 1.6 to 20.2 pmol FR/mg protein, and this new cell line was renamed 4T1-pico (Table 2).

When tumors of the 3 cell lines were generated in BALB/c mice and FR levels were quantified, FR expression was found to be the lowest in 4T1 tumors (1.5 pmol FR/mg protein) and the highest in M109 tumors (22.9 pmol FR/mg protein) as expected, whereas the 4T1-pico tumors expressed 7.2 pmol FR/mg of protein. Based on these differential levels of membrane-associated FR expression, 4T1, 4T1-pico, and M109 cells were used as tumor models for the assessment of ^{99m}Tc-EC20 uptake.

As shown in Table 2, the net uptake of radiolabel in each of these tumors was proportional to their respective FR levels. Thus, M109 tumors accumulated the greatest amount (15.5 %ID/g), whereas the 4T1-pico tumors accumulated much less (8.71 %ID/g). The 4T1 tumors (derived from cells that express the lowest quantity of FR) accumulated the lowest amount of radiolabel (2.6 %ID/g). Importantly, uptake of ^{99m}Tc-EC20 was reduced to background levels

TABLE 1
Biodistribution of ^{99m}Tc-EC20 and ^{99m}Tc-EC53

	^{99m}Tc-EC20		^{99m}Tc-EC53	
Organ	%ID/g	T/NT	%ID/g	T/NT
Blood	0.27 ± 0.05	67.2 ± 5.6	0.38 ± 0.03	31.4 ± 13.7
Heart	1.97 ± 0.28	9.1 ± 0.9	1.09 ± 0.28	12.2 ± 8.2
Lung	2.39 ± 0.56	7.6 ± 1.3	0.89 ± 0.30	15.3 ± 10.4
Liver	3.48 ± 0.96	5.2 ± 0.8	3.86 ± 0.96	3.4 ± 2.2
Intestine	4.89 ± 1.37	3.7 ± 0.6	3.53 ± 0.86	3.6 ± 2.0
Kidney	116.46 ± 14.17	0.2 ± 0.01	77.99 ± 6.19	0.2 ± 0.1
Muscle	1.70 ± 0.70	11.3 ± 3.8	0.76 ± 0.31	17.1 ± 7.0
Spleen	0.46 ± 0.11	39.5 ± 7.5	0.67 ± 0.22	17.7 ± 2.4
Tumor	17.68 ± 1.95	—	11.77 ± 4.26	—
Stomach	1.47 ± 0.08	12.1 ± 0.8	1.04 ± 0.36	12.6 ± 7.3

Imaging agents were injected intravenously into BALB/c mice on folate-deficient diet bearing subcutaneous M109 tumors, and animals were necropsied 4 h later. Values are means ± SD (n = 3).

TABLE 2
Dependency of ^{99m}Tc-EC20 Tumor Uptake on FR Density

Cell line	FR expression* (pmol/mg protein)		^{99m}Tc-EC20 uptake (%ID/g tissue)	
	Cells	Tumors	EC20	EC20 + 100 × FA
4T1	1.6	1.5	2.58 ± 0.68	0.30 ± 0.05
4T1-pico	20.2	7.2	8.71 ± 2.25	0.50 ± 0.05
M109	95.5	22.9	15.53 ± 1.90	0.61 ± 0.05

*N = 1; however, typical errors for such measurements are <10%.
FA = folic acid.
Values are means ± SD (n = 3).

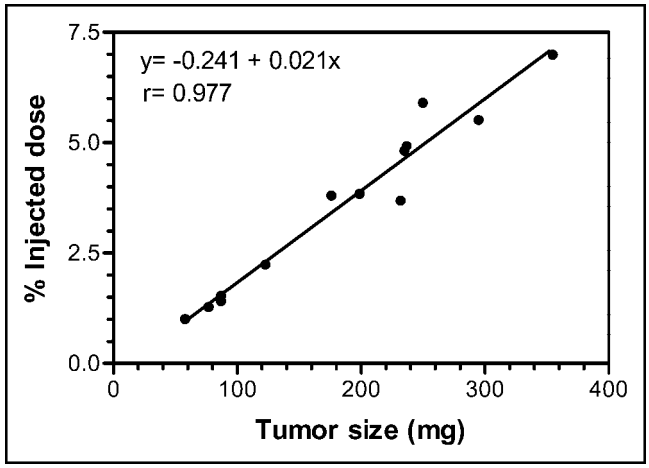

FIGURE 5. ^{99m}Tc-EC20 uptake in M109 tumors of varying sizes. BALB/c mice bearing M109 tumors received an intravenous dose of 50 μg/kg EC20 (67 nmol/kg) in approximately 0.1 mL PBS during brief diethyl ether anesthesia. At designated times after injection, each animal was killed by CO_2 asphyxiation, and tumors were collected and counted for associated radioactivity.

(<1 %ID/g) in all 3 tumor types when a competable excess of free folic acid was coinjected, thus indicating that tumor uptake was primarily due to the presence of the FR.

Effect of Tumor Size on ^{99m}Tc-EC20 Uptake by M109 Tumors

A large tumor load is usually associated with decreased therapeutic efficacy. One reasonable explanation for this observation is that the tumor cells located deep within the malignant tissue become less accessible to parenterally administered drugs. In an attempt to relate tumor size with ^{99m}Tc-EC20 uptake, we retrospectively analyzed the results of 4 different M109 biodistribution experiments. The majority of the tumors from these studies were found to be in the range of 50–400 mm^3 (i.e., well established). Notably, mice bearing tumors with a size of <50 mm^3 were excluded from evaluation since tumors that are barely palpatable are often difficult to excise without some associated normal connective tissue. The data from the various experiments were compiled, and the %ID of ^{99m}Tc-EC20 within each tumor was plotted against the respective tumor size. As shown in Figure 5, the %ID of ^{99m}Tc-EC20 in the tumors is very well correlated (r = 0.977) with the size of the tumor. From this analysis we concluded that as the tumor size increases, tumor-associated FRs remain readily accessible to blood-borne folate-drug conjugates. Interestingly, the data also suggest that the net amount of FR expressed per gram of tumor does not decrease as the disease progresses.

Uptake of ^{99m}Tc-EC20 as a Consequence of Diet Modulation

Folic acid–deficient diets have traditionally been used on mouse models when investigating FR targeting. Although no apparent adverse effects occur with their use, many have wondered if alternative diets could be used. Within this study, we investigated the effect of feeding mice a leucovorin (5-formyltetrahydrofolate)-supplemented diet on the tumor-targeting ability of ^{99m}Tc-EC20 (*25*). Thus, mice were maintained on a diet supplemented with 0.5 mg of leucovorin per kilogram of chow for a total of 5 wk before biodistribution studies were performed. Based on a food intake of 3-g chow per day for an average 20-g laboratory mouse, roughly 1.5 μg of leucovorin supplement would be ingested (75 μg/kg body weight, or 227 μg/m^2 of body-surface area). Notably, the U.S. Department of Agriculture (USDA)–recommended daily allowance for folate is ~400 μg/d per human (5.7 μg/kg, or ~235 μg/m^2 body-surface area). Thus, the 0.5-mg leucovorin/kg chow was expected to deliver the USDA–recommended folate equivalent to the mice, based on body-surface area normalization.

As shown in Table 3, the biodistribution pattern for mice on a leucovorin-supplemented diet was essentially identical with the distribution pattern in the folate-deficient diet (Table 1). Neither diet significantly affected the uptake of ^{99m}Tc-EC20 in the FR–positive tumors or kidneys (17.7 vs.

TABLE 3
Biodistribution and T/NT Tissue Ratios in M109 Tumor-Bearing BALB/c Mice Fed Leucovorin-Supplemented Folate-Deficient Diets

Organ	Folate-deficient diet + leucovorin	
	%ID/g	T/NT
Blood	0.26 ± 0.07	67.67 ± 7.40
Heart	2.20 ± 0.06	7.83 ± 1.75
Lung	1.58 ± 0.19	10.79 ± 1.46
Liver	4.22 ± 0.04	4.08 ± 1.00
Intestine	3.04 ± 2.04	7.12 ± 3.96
Kidney	109.90 ± 12.78	0.16 ± 0.04
Muscle	1.99 ± 0.39	8.64 ± 1.11
Spleen	0.44 ± 0.07	38.72 ± 3.98
Tumor	17.24 ± 4.22	—
Stomach	1.43 ± 0.07	12.08 ± 2.95

Values are means ± SD (n = 3). BALB/c mice weighed 20 ± 2 g.

17.2 %ID/g in tumor and 116.5 vs. 109.9 %ID/g in kidney from mice fed the folate-deficient and leucovorin-supplemented diets, respectively). These data suggest that neither leucovorin nor its metabolites substantially competed with ^{99m}Tc-EC20 (a folate conjugate) for binding to the FR.

Effect of Dose Administration Route and Tumor Location on ^{99m}Tc-EC20 Biodistribution

One major advantage of intraperitoneal versus intravenous dosing is that intraperitoneally resident tumors (e.g., ovarian cancer) can be quickly exposed to high localized drug concentrations. Although this benefit is obvious for a nontargeted drug whose entry into a cell is concentration dependent, the benefit for administering an FR–targeted (and saturable) molecule intraperitoneally has yet to be determined. To better understand the advantages and limitations of in vivo folate targeting, we believed it was necessary to study the uptake of a model folate conjugate (^{99m}Tc-EC20) into FR–positive tumors as a function of tumor location as well as route of dose administration.

Using mice bearing either subcutaneous M109 tumor implants or clearly identifiable and excisable intraperitoneal M109 tumor nodules, an experiment was conducted to compare the tissue biodistribution of ^{99m}Tc-EC20 after either intravenous or intraperitoneal administration. As shown in Table 4, uptake of the folate-targeted imaging agent into intraperitoneal tumors was independent of the dosing route. Thus, intravenous and intraperitoneal routes of administration enabled the capture of ^{99m}Tc-EC20 at 17.1 and 16.2 %ID/g of intraperitoneal tumor, respectively. Other intraperitoneally resident tissues—such as intestine, stomach, spleen, liver, and kidney—displayed similar (but low) uptake of the targeted imaging agent after either intraperitoneal or intravenous dosing. Likewise, the biodistribution pattern of ^{99m}Tc-EC20 in animals bearing subcutaneous tumors was apparently independent of the dosing route. Thus, intravenous and intraperitoneal routes of administration enabled the capture of EC20 at 17.2 and 18.8 %ID/g of subcutaneous tumor, respectively. We conclude from this study that FR–positive tumors in our murine model can be equally accessed by folate-targeted agents in a manner that is independent of both the tumor location and the route of dose administration.

Effect of Predosed and Codosed Folic Acid with ^{99m}Tc-EC20

In an effort to improve the tumor-to-background ratio, we have investigated the effect of injecting unconjugated folic acid before or during the dosing of ^{99m}Tc-EC20. Thus, 1 or 10 eq. of folic acid were injected either 15 min before the dosing of ^{99m}Tc-EC20 or together as a single formulation. As shown in Table 5, the addition of folic acid decreased the uptake of ^{99m}Tc-EC20 into tumors in a dose-dependent manner. Tumor uptake was reduced from 24.7 to 16.51 %ID/g with the codose and reduced to 16.47 %ID/g with the predose of 1 eq. of folic acid, whereas tumor uptake was reduced to 4.65 %ID/g with the codose and reduced to 5.0 %ID/g with the predose of 10 eq. of folic acid. Interestingly, T/NT ratios increased 1.6- to 2.7-fold for every nontarget organ when ^{99m}Tc-EC20 was codosed with 1 eq. of folic acid. For example, the tumor-to-blood ratio increased from 79.6 to 213.6, and the tumor-to-muscle ratio increased from 13.6 to 36.7. T/NT ratios also increased in every organ when the mice were predosed with the 1 eq. of folic acid, albeit to a lesser extent, except in the case of spleen, where the ratio remained the same. When the mice were codosed with 10 eq. of folic acid, T/NT ratios were higher in the case of blood, heart, lung, and muscle as compared with similar ratios from animals dosed with ^{99m}Tc-EC20 alone. However, since codosing ^{99m}Tc-EC20 with 1 eq. of folic acid gave the highest T/NT ratios, especially with respect to all organs in the peritoneal region, we concluded that this dosing manipulation would yield the best tumor-to-back-

TABLE 4
Biodistribution of ^{99m}Tc-EC20

Organ	Subcutaneous tumor		Intraperitoneal tumor*	
	Intravenous dose	Intraperitoneal dose	Intravenous dose	Intraperitoneal dose
Blood	0.26 ± 0.07	0.28 ± 0.06	0.38 ± 0.23	0.18 ± 0.02
Heart	2.20 ± 0.06	2.62 ± 0.50	1.34 ± 0.35	1.75 ± 0.42
Lung	1.58 ± 0.19	2.25 ± 0.37	1.46 ± 1.14	1.20 ± 0.13
Liver	4.22 ± 0.04	4.29 ± 0.71	4.67 ± 1.42	3.19 ± 0.15
Intestine	3.04 ± 2.04	2.64 ± 1.26	3.10 ± 2.24	2.77 ± 1.66
Kidney	109.90 ± 12.8	98.78 ± 6.9	125.96 ± 15.5	105.65 ± 11.1
Muscle	1.99 ± 0.39	1.90 ± 0.32	1.79 ± 0.80	1.39 ± 0.57
Spleen	0.44 ± 0.07	0.51 ± 0.13	1.81 ± 1.76	0.69 ± 0.15
Tumor	17.24 ± 4.22	18.77 ± 5.12	17.07 ± 3.39	16.24 ± 1.32
Stomach	1.43 ± 0.07	1.48 ± 0.12	1.49 ± 1.46	1.83 ± 0.88

*Each intraperitoneal tumor is sum of 4–6 tumor nodules (30–60 mg each).

BALB/c mice (weight, 20 ± 2 g) bearing subcutaneous or intraperitoneal tumors were injected intravenously or intraperitoneally with ^{99m}Tc-EC20 and then necropsied after 4 h. Values are the means ± SD (n = 3).

TABLE 5
Biodistribution Data and T/NT Tissue Ratios in M109 Tumor-Bearing BALB/c Mice Injected with ^{99m}Tc-EC20 With or Without Free Folic Acid

			^{99m}Tc-EC20 + 1 eq. FA				^{99m}Tc-EC20 + 10 eq. FA			
	^{99m}Tc-EC20		Codose		Predose		Codose		Predose	
Organ	%ID/g	T/NT	%ID/g	T/NT	%ID/g	T/NT	%ID/g	T/NT	%ID/g	T/NT
Blood	0.32 ± 0.11	79.6 ± 15	0.08 ± 0.01	213.6 ± 87	0.12 ± 0.06	148.0 ± 39	0.05 ± 0.01	98.2 ± 17	0.05 ± 0.02	111.3 ± 63
Heart	1.89 ± 0.41	13.4 ± 3.5	0.72 ± 0.09	23.0 ± 5.7	0.90 ± 0.40	20.2 ± 7.8	0.29 ± 0.02	16.3 ± 2.7	0.26 ± 0.05	19.4 ± 2.7
Lung	2.00 ± 0.54	13.2 ± 5.7	0.67 ± 0.04	24.8 ± 7.5	0.73 ± 0.14	22.7 ± 1.3	0.23 ± 0.03	20.5 ± 6.5	0.27 ± 0.02	18.6 ± 3.8
Liver	4.70 ± 1.01	5.3 ± 0.7	1.84 ± 0.39	9.3 ± 3.3	2.86 ± 0.20	5.7 ± 0.6	1.63 ± 0.18	2.9 ± 0.4	1.92 ± 0.57	2.8 ± 1.3
Spleen	0.56 ± 0.07	44.7 ± 12	0.24 ± 0.01	70.0 ± 18.1	0.40 ± 0.11	43.5 ± 15.3	0.28 ± 0.03	17.0 ± 4.2	0.41 ± 0.09	12.9 ± 4.9
Intestine	3.91 ± 1.34	6.6 ± 1.8	1.12 ± 0.45	17.9 ± 12.4	2.03 ± 1.34	11.4 ± 7.8	1.88 ± 0.28	2.6 ± 0.9	1.34 ± 1.18	7.5 ± 7.7
Kidney	175.2 ± 15	0.1 ± 0.03	100.9 ± 16	0.2 ± 0.1	132.7 ± 20	0.1 ± 0.03	41.93 ± 6.2	0.1 ± 0.01	54.30 ± 1.8	0.1 ± 0.01
Muscle	1.80 ± 0.21	13.6 ± 2.0	0.48 ± 0.13	36.7 ± 15.9	0.82 ± 0.16	20.3 ± 4.2	0.18 ± 0.05	26.5 ± 3.3	0.30 ± 0.06	17.3 ± 4.3
Stomach	1.45 ± 0.37	18.5 ± 9.6	0.55 ± 0.12	30.0 ± 2.1	0.56 ± 0.26	35.7 ± 22.0	0.26 ± 0.03	18.1 ± 3.4	0.36 ± 0.08	14.3 ± 3.2
Tumor	24.66 ± 5.9	—	16.51 ± 4.6	—	16.47 ± 2.7	—	4.65 ± 0.85	—	5.00 ± 0.72	—

FA = folic acid.
Values are means ± SD (n = 3).

ground contrast at the typical radiopharmaceutical dose level used.

DISCUSSION

We previously described the synthesis and characterization of a novel ^{99m}Tc-based folate-peptide chelator called EC20 (*23*). This agent was found to bind FR–positive cells and tissues with high affinity and was deemed useful for radiodiagnostic applications. EC20 consists of a pteroic acid moiety that is covalently attached to a tetrapeptide chelate. The peptide contains one D-Glu residue in place of the natural L-Glu residue within folate (Pte-Glu), whereas all remaining amino acid residues are in the L-configuration. As stated earlier, serum peptidases can be problematic for peptide-based pharmaceuticals, and substitution of the natural L-amino acid residues with corresponding D-enantiomers can often improve an agent's serum stability profile. Thus, in the beginning of our investigation, we elected to synthesize and evaluate the biologic properties of an all-D-EC20 analog, called EC53.

^{99m}Tc-EC20 and ^{99m}Tc-EC53 were evaluated in M109 tumor-bearing BALB/c mice, and both agents were found to have similar patterns of tissue biodistribution. Unexpectedly, the net uptake of ^{99m}Tc-EC53 in FR–positive tumor and kidney was actually ~33% lower compared with ^{99m}Tc-EC20. However, this finding was attributed to the measured lower affinity that EC53 has for the FR (Fig. 4). From these results we concluded that D-amino acid substitutions (in the β-Dpr-Asp-Cys locus of EC20) did not afford any biologic advantage for in vivo FR targeting.

It has been previously demonstrated that the uptake of folate-targeted biomolecules in cell culture is roughly proportional to the FR density on the cell membranes (*9*,*26*). However, in vivo tumor uptake of a folate ligand presumably depends not only on FR expression levels but also on the tumor microenvironment. To address this issue, we first examined the uptake of ^{99m}Tc-EC20 into murine tumors that expressed various levels of the FR protein. We found that the net uptake of radiolabel in each of these tumors was proportional to their respective FR expression levels. Since tumor size can possibly influence drug accumulation, we next studied the relationship between ^{99m}Tc-EC20 uptake and tumor mass. Notably, a large tumor load could decrease the therapeutic efficacy of drugs by various mechanisms. In fact, many solid tumors have poorly formed vasculatures with intermittent blood flow and large distances between functional blood vessels (*27*). Further, in the center of large tumors, increased interstitial pressure gradients cause radial fluid flow from the center to the periphery (*28*). To reach all of the cells in a tumor, the agent must penetrate through multiple layers of solid tissue, and this requirement may represent a formidable barrier to many therapeutics. For ^{99m}Tc-EC20, we found that its tumor penetration was not significantly different among tumors of widely varying sizes. More specifically, there was a consistent increase in the relative amount of ^{99m}Tc-EC20 in the tumor as a function of tumor size over the range of 50–400 mm^3. Taken together, these data confirm that folate conjugates can readily penetrate deeply into solid FR–positive tumors, and the net uptake is apparently proportional to the tumor's size.

It has been shown that nontargeted drugs, such as methotrexate and cisplatin, are retained for prolonged periods of time within the peritoneal cavity after intraperitoneal administration (*29*). This enables an intraperitoneal tumor to be exposed to higher drug concentrations, thus increasing the potential for enhanced antitumor activity. When dosed at 50 nmol/kg, the amount of ^{99m}Tc-EC20 found in the tumor was very similar when the agent was administered either intraperitoneally or intravenously (irrespective of the tumor location). There were also no significant differences in uptake of ^{99m}Tc-EC20 within the kidneys and other abdominally localized tissues after either intraperitoneal or intravenous administration. These results indicate that there is no advantage in administering ^{99m}Tc-EC20 intraperitone-

ally compared with intravenously and further suggests that the main entry of this agent into tissues is vascular.

It is noteworthy that standard laboratory chows are extensively supplemented with folic acid (typically 6 mg/kg of chow). This causes laboratory animals to have high basal plasma and tissue folate levels (*16*). In fact, mice fed such diets have plasma folate levels of 300–800 nmol/L, which is 15- to 40-fold higher than that measured in human plasma. These supraphysiologic levels of plasma folate will compete with folate-drug conjugates for FR binding and possibly tumor uptake. Thus, most laboratories that study folate/antifolate or folate-conjugate pharmacology have often used a nonfolate–supplemented laboratory chow. In some cases, 1% of the succinylsulfathiazole antibiotic is included into the chow formulation to kill folate-producing intestinal flora. However, we have noted that mice fed such chows are not as healthy or active as those animals that are fed diets lacking the antibiotic.

To the best of our knowledge and experience, use of a folate-free chow (antibiotic free) enables the lowering of serum folate levels to more physiologically relevant levels (~50 nmol/L) without causing any concomitant adverse effects (*16*). However, because folate deficiency has been implicated in multiple disorders—such as atherosclerotic cardiovascular disease, neurologic disorders, congenital defects, and carcinogenesis (*30–32*)—and the safety of animals kept on such diets for long periods is unknown, we searched for an alternative chow that might maintain tissue folate levels without significantly interfering with a folate conjugate's ability to target tumor-associated FRs. We hypothesized that substituting folic acid in the chow with a compound such as leucovorin (folinic acid) should maintain similar plasma folate pools as folic acid (*25*) and, therefore, satisfy the tissue folate needs in animals enduring long-term FR–targeted therapy. The difference, though, is that leucovorin (and other reduced folates) is a good substrate for the reduced folate transport carrier, but it has low affinity for the FR; thus, leucovorin—and any quantity thereof that may have been methylated within the intestine before release into the plasma—will not effectively compete with folate-conjugate binding to the FR (*33*). Therefore, we custom formulated a nonfolate–supplemented chow with 0.5 mg leucovorin per kilogram, which incidentally was expected to deliver the USDA–recommended folate equivalent to the mice (based on body-surface area normalization). Indeed, our experimental results indicated that mice fed the leucovorin-supplemented diet looked and behaved normally, and their serum folate levels were measured at 62 nmol/L after 3 wk. In addition, the net ^{99m}Tc-EC20 uptake in FR–expressing tumors was nearly identical to the tumor uptake levels of mice fed the common nonfolate–supplemented chow. Although it was not specifically assessed here, these results suggested that leucovorin-supplemented diets could be beneficial to the animal's well being when treated for extended periods of time with folate-drug conjugates. Likewise, clinical applications are possible since leucovorin is commonly administered to cancer patients, albeit for a different purpose (*34*,*35*).

Recent evidence has shown that the presence of a critical mass of unlabeled peptide significantly improves the uptake of peptide-based radioligands at the target tissue in both experimental animals and patients (*1*). Although we predicted that a similar approach would have a negative effect on the uptake of ^{99m}Tc-EC20 in tumors, we elected to coadminister ^{99m}Tc-EC20 to tumor-bearing animals in various combinations with free folic acid. As expected, our results confirmed that the percentage uptake of ^{99m}Tc-EC20 in FR–positive tumors was optimal when folic acid was absent from the formulation. However, we did discover that higher T/NT uptake ratios were obtained when a single equivalent of free folic acid was coadministered with the ^{99m}Tc-EC20. This finding might be the result of low levels of FRs in blood and some nontarget tissues that become at least partially saturated by the coformulated free folic acid; thus, only the more highly expressing FR–positive organs (tumor and kidney) would be available to bind ^{99m}Tc-EC20 under these dosing conditions. The implication of this result is that the sensitivity (contrast) of detecting FR–positive tumors might be improved by varying the mass of free folic acid in the radiotracer formulation.

CONCLUSION

In summary, the net tumor uptake of ^{99m}Tc-EC20 was found to be specific and proportional to FR expression levels in tumor cells as well as linear with respect to overall tumor size. Its uptake was found to be independent of solid tumor location (intraperitoneal vs. subcutaneous) and the route of administration (intraperitoneal vs. intravenous), and T/NT ratios could be improved up to 2.7-fold when 1 eq. of free folic acid was coinjected with ^{99m}Tc-EC20. Together with the observation that the net tumor uptake of its all-D-isomeric counterpart (EC53) was lower, these data suggest that ^{99m}Tc-EC20 may be a clinically useful, noninvasive radiodiagnostic agent for detecting the locus of FR–positive cancers.

ACKNOWLEDGMENT

We thank Dr. Philip S. Low for his valuable discussions.

REFERENCES

1. Breeman WA, de Jong M, Kwekkeboom DJ, et al. Somatostatin receptor-mediated imaging and therapy: basic science, current knowledge, limitations and future perspectives. *Eur J Nucl Med.* 2001;28:1421–1429.
2. Taillefer R. The role of ^{99m}Tc-sestamibi and other conventional radiopharmaceuticals in breast cancer diagnosis. *Semin Nucl Med.* 1999;29:16–40.
3. Weitman SD, Lark RH, Coney LR, et al. Distribution of the folate receptor GP38 in normal and malignant cell lines and tissues. *Cancer Res.* 1992;52:3396–3401.
4. Ross JF, Chaudhuri PK, Ratnam M. Differential regulation of folate receptor isoforms in normal and malignant tissues in vivo and in established cell lines: physiologic and clinical implications. *Cancer.* 1994;73:2432–2443.
5. Toffoli G, Cernigoi C, Russo A, Gallo A, Bagnoli M, Boiocchi M. Overexpression of folate binding protein in ovarian cancers. *Int J Cancer.* 1997;74:193–198.
6. Leamon CP, Low PS. Delivery of macromolecules into living cells: a method that exploits folate receptor endocytosis. *Proc Natl Acad Sci USA.* 1991;88:5572–5576.

7. Leamon CP, Low PS. Folate-mediated targeting: from diagnostics to drug and gene delivery. *Drug Discov Today.* 2001;6:44–51.
8. Reddy JA, Low PS. Folate-mediated targeting of therapeutic and imaging agents to cancers. *Crit Rev Ther Drug Carrier Syst.* 1998;15:587–627.
9. Leamon CP, Pastan I, Low PS. Cytotoxicity of folate-Pseudomonas exotoxin conjugates toward tumor cells: contribution of translocation domain. *J Biol Chem.* 1993;268:24847–24854.
10. Rund LA, Cho BK, Manning TC, Holler PD, Roy EJ, Kranz DM. Bispecific agents target endogenous murine T cells against human tumor xenografts. *Int J Cancer.* 1999;83:141–149.
11. Lu Y, Low PS. Folate targeting of haptens to cancer cell surfaces mediates immunotherapy of syngeneic murine tumors. *Cancer Immunol Immunother.* 2002;51:153–162.
12. Lee RJ, Low PS. Delivery of liposomes into cultured KB cells via folate receptor-mediated endocytosis. *J Biol Chem.* 1994;269:3198–3204.
13. Reddy JA, Dean D, Kennedy MD, Low PS. Optimization of folate-conjugated liposomal vectors for folate receptor-mediated gene therapy. *J Pharm Sci.* 1999; 88:1112–1118.
14. Reddy JA, Abburi C, Hofland H, et al. Folate-targeted, cationic liposome-mediated gene transfer into disseminated peritoneal tumors. *Gene Ther.* 2002;9: 1542–1550.
15. Wang S, Lee RJ, Mathias CJ, Green MA, Low PS. Synthesis, purification, and tumor cell uptake of ^{67}Ga-deferoxamine–folate, a potential radiopharmaceutical for tumor imaging. *Bioconjug Chem.* 1996;7:56–62.
16. Mathias CJ, Wang S, Lee RJ, Waters DJ, Low PS, Green MA. Tumor-selective radiopharmaceutical targeting via receptor-mediated endocytosis of gallium-67-deferoxamine-folate. *J Nucl Med.* 1996;37:1003–1008.
17. Wang S, Luo J, Lantrip DA, et al. Design and synthesis of [^{111}In]DTPA-folate for use as a tumor-targeted radiopharmaceutical. *Bioconjug Chem.* 1997;8:673–679.
18. Mathias CJ, Wang S, Waters DJ, Turek JJ, Low PS, Green MA. Indium-111-DTPA-folate as a potential folate-receptor-targeted radiopharmaceutical. *J Nucl Med.* 1998;39:1579–1585.
19. Liu S, Edwards DS. ^{99m}Tc-Labeled small peptides as diagnostic radiopharmaceuticals. *Chem Rev.* 1999;99:2235–2268.
20. Guo W, Hinkle GH, Lee RJ. ^{99m}Tc-HYNIC-folate: a novel receptor-based targeted radiopharmaceutical for tumor imaging. *J Nucl Med.* 1999;40:1563–1569.
21. Ilgan S, Yang DJ, Higuchi T, et al. ^{99m}Tc-Ethylenedicysteine-folate: a new tumor imaging agent—synthesis, labeling and evaluation in animals. *Cancer Biother Radiopharm.* 1998;13:427–435.
22. Mathias CJ, Hubers D, Low PS, Green MA. Synthesis of [^{99m}Tc]DTPA-folate and its evaluation as a folate-receptor-targeted radiopharmaceutical. *Bioconjug Chem.* 2000;11:253–257.
23. Leamon CP, Parker MA, Vlahov IR, et al. Synthesis and biological evaluation of EC20: a new folate-derived, ^{99m}Tc-based radiopharmaceutical. *Bioconjug Chem.* 2002;13:1200–1210.
24. Westerhof GR, Schornagel JH, Kathmann I, et al. Carrier- and receptor-mediated transport of folate antagonists targeting folate-dependent enzymes: correlates of molecular-structure and biological activity. *Mol Pharmacol.* 1995;48:459–471.
25. Schmitz JC, Stuart RK, Priest DG. Disposition of folic acid and its metabolites: a comparison with leucovorin. *Clin Pharmacol Ther.* 1994;55:501–508.
26. Reddy JA, Low PS. Enhanced folate receptor mediated gene therapy using a novel pH-sensitive lipid formulation. *J Control Release.* 2000;64:27–37.
27. Jain RK. Vascular and interstitial barriers to delivery of therapeutic agents in tumors. *Cancer Metastasis Rev.* 1990;9:253–266.
28. Jain RK. Delivery of novel therapeutic agents in tumors: physiological barriers and strategies. *J Natl Cancer Inst.* 1989;81:570–576.
29. Pestieau SR, Stuart OA, Sugarbaker PH. Multi-targeted antifolate (MTA): pharmacokinetics of intraperitoneal administration in a rat model. *Eur J Surg Oncol.* 2000;26:696–700.
30. Stanger O. Physiology of folic acid in health and disease. *Curr Drug Metab.* 2002;3:211–223.
31. Donnelly JG. Folic acid. *Crit Rev Clin Lab Sci.* 2001;38:183–223.
32. Hall JG, Solehdin F. Folate and its various ramifications. *Adv Pediatr.* 1998;45: 1–35.
33. Huennekens FM, Vitols KS, Henderson GB. Transport of folate compounds in bacterial and mammalian cells. *Adv Enzymol Relat Areas Mol Biol.* 1978;47: 313–346.
34. Leichman CG, Fleming TR, Muggia FM, et al. Phase II study of fluorouracil and its modulation in advanced colorectal cancer: a Southwest Oncology Group study. *J Clin Oncol.* 1995;13:1303–1311.
35. Levin RD, Gordon JH. Fluorodeoxyuridine with continuous leucovorin infusion: a phase II clinical trial in patients with metastatic colorectal cancer. *Cancer.* 1993;72:2895–2901.